Ultrastructural Studies of the Squid Nerve Fibers

GLORIA M. VILLEGAS and RAIMUNDO VILLEGAS

From Centro de Biofísica, Instituto Venezolano de Investigaciones Científicas (IVIC), Caracas, Venezuela

The work of Young (1) on the anatomy of the squid nervous system revealed the existence of giant nerve fibers suitable for exploring the fundamental mechanisms of nerve function. Geren and Schmitt (2) made the first electron microscopic observations of these fibers. Our work has been concerned with the study of the functional organization of these giant nerve fibers (3–6).

The present paper deals with three different problems: (*a*) the general structure in the different species of squid used, (*b*) the nature of the pathways located in the Schwann cell layer, and (*c*) the structure of the axolemma.

GENERAL STRUCTURE

Three species of squid have been examined with the electron microscope. They are *Dorytheutis plei* and *Sepioteuthis sepioidea* from the Caribbean Sea and *Dosidicus gigas* from the Pacific Ocean.

The giant nerve fiber of the first stellar nerve presents an axon 200–500 μ in diameter in the tropical species, and about 800–1200 μ in diameter in *D. gigas*. In this latter species, as previously described for the other species (3–5), the axoplasm consists of bundles of filaments 50–70 A thick and, scattered among them, rows of smooth membranous vesicles and some large cisterns of the endoplasmic reticulum. Mitochondria appear in concentrations of about 40 per 100 μ^2 at the peripheral axoplasm, and about 30 per 100 μ^2 in deeper regions. They are elongated bodies, 0.2–0.4 μ thick, with their major axes, up to 3 μ long orientated longitudinally. About 25% of the most peripherally situated mitochondria are rounded and have diameters over 0.4 μ.

The Schwann cell layer of the giant nerve fiber is formed by several Schwann cells arranged in a single row around the axon (Fig. 1 *a*). Each Schwann cell is 0.2–0.8 μ thick in the squid *D. plei* (3), while in the *S. sepioidea* and *D. gigas* it is about 1.5–6 μ in thickness. In the latter species, the cytoplasm of the Schwann cell, especially in the perinuclear region, contains numerous membranous vesicles. The nucleus does not differ in aspect from the other squid species studied (3).

The Schwann layer is crossed by tortuous channels which represent intercellular spaces between two neighbor cells or between two processes of the same cell (6). A thick basement membrane, about 0.2 μ in thickness, covers the external surface of the Schwann cells, and, especially in *S. sepioidea* and *D. gigas*, deeply invaginates

these outer surfaces. In the tropical species studied, the basement membrane consists of a homogenous, medium dense material, while in the *D. gigas*, the membrane is formed by 200-A thick fibrils grouped in tight bundles, parallel to the Schwann cell surface, in the inner region of the basement membrane (Fig. 2). At the outer region the fibrils are loosely intermingled. In each of the three species examined, there exists, outside the basement membrane, a zone 0.3–0.8 μ thick, where islets of a homogenous, dense material are observed, as well as some collagen fibrils. This zone separates the basement membrane from the alternated layers of connective tissue cells and fibrils forming the endoneurium.

Farther out of the endoneurium lie bundles of small nerve fibers which could be classified according to their size and glial relationship as follows. (*a*) A type with axons 1.5–10 μ in diameter, usually ensheathed by only one Schwann cell (Fig. 1 *b*, and Fig. 4). However, two or three Schwann cells have been observed sometimes surrounding the largest fibers of this type. (*b*) A second type corresponds to small

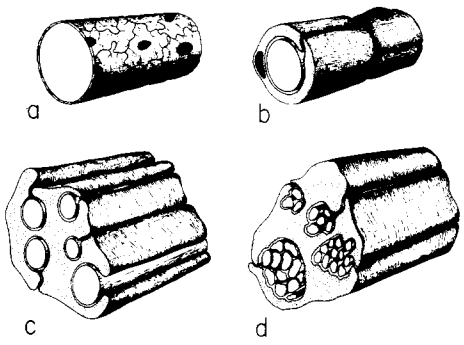

FIGURE 1. Scheme representing the four different types of nerve fibers found in the stellar nerve of the squid. At *a*, the giant fiber with the axon surrounded by several Schwann cells. At *b*, the medium-sized fiber with the axon, 1.5–10 μ in diameter, ensheathed by one Schwann cell. At *c*, the small fibers with several axons, 0.5–1 μ in diameter, surrounded by one Schwann cell. At *d*, the minute fibers with bundles of axons, less than 0.5 μ in diameter, ensheathed by one Schwann cell.

fibers 0.5–1 μ in diameter, grouped in bundles enveloped by only one Schwann cell (Fig. 1 *c*). Each fiber is separated from its neighbors by glial cytoplasm. This pattern is similar to that of the vertebrate unmyelinated fibers (7). (*c*) Finally, the last type is represented by minute fibers, less than 0.5 μ in diameter, forming large bundles ensheathed by one Schwann cell (Fig. 1 *d* and Fig. 3). In each bundle, the axons are apposed membrane to membrane without intervening glial cytoplasm. This arrangement is similar to the one described in the olfactory nerve (8). The basement membrane covering the Schwann cell of the three types of small fibers is about 150–300 A thick.

NATURE OF THE PATHWAYS LOCATED IN THE SCHWANN CELL LAYER

To study the permeability of the pathways crossing the Schwann cell layer, we investigated, with the aid of the electron microscope, the diffusion of an electron-opaque substance (9). These pathways are the mesaxon gaps in the small nerve fibers and

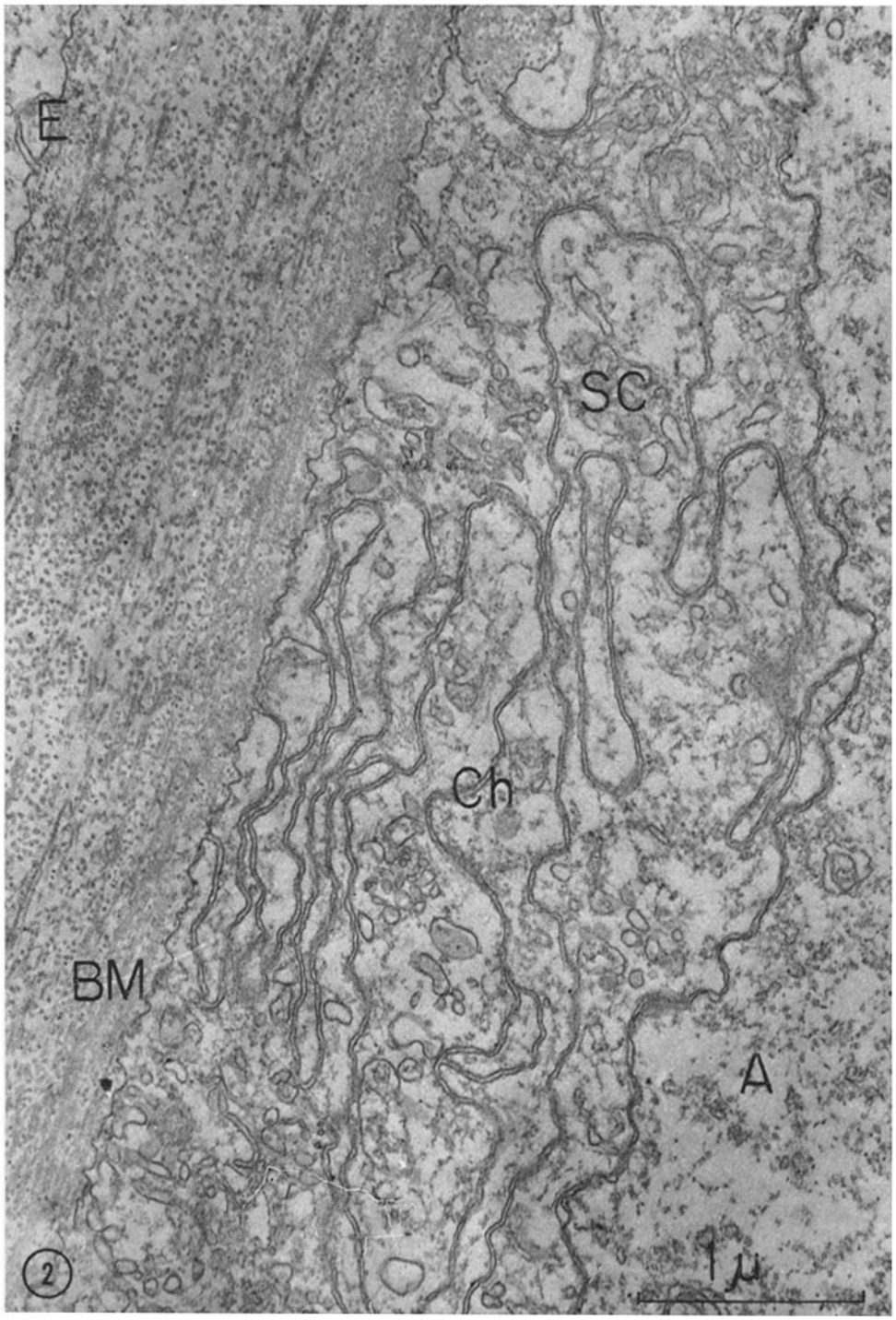

FIGURE 2. Electron micrograph of the *D. gigas* giant fiber. Cross-section showing part of the axon (*A*), the Schwann cell layer (*SC*) crossed by channels (*Ch*) and covered at the outer surface by the basement membrane (*BM*). A fibrous dense material forms the basement membrane and appears loosely intermingled with connective tissue fibrils towards the layered endoneurium (*E*). OsO_4-fixed, Epon-embedded material.

the Schwann-layer channels in the giant nerve fiber. Artificial sea water containing thorium dioxide (thorotrast) was used as incubating medium.

Action potentials elicited by electrical stimulation were recorded before and after 1 hr incubation. That the electron microscope examination demonstrated pinocytotic vesicles in the Schwann cells and axons also accounts for a sign of vital activity during the incubation (Fig. 3). In the small nerve fibers the concentration of thorium parti-

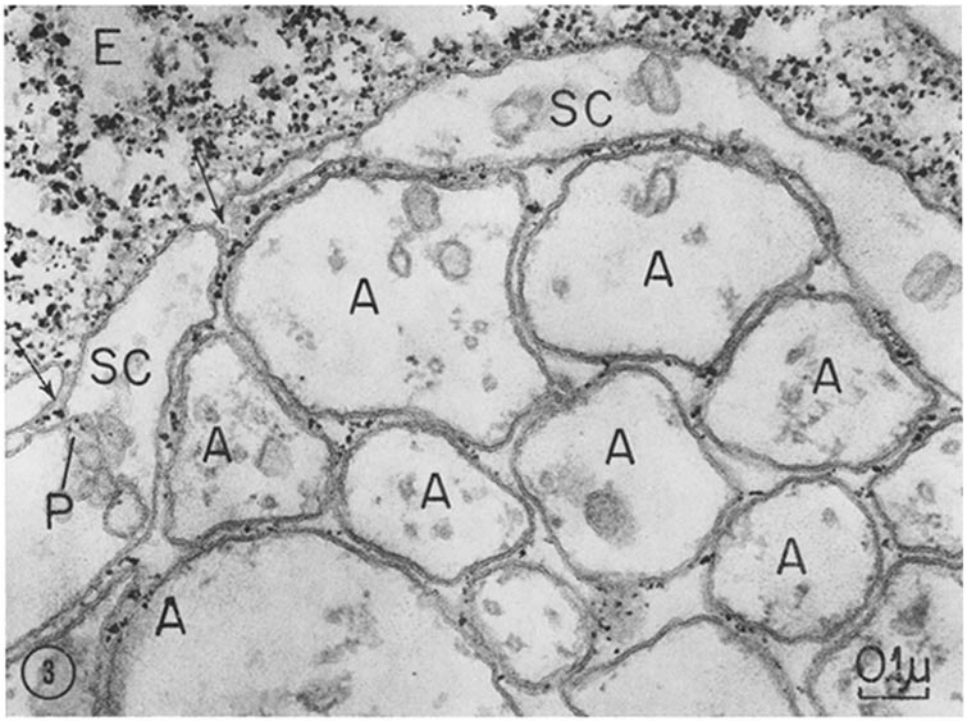

FIGURE 3. Electron micrograph of *D. plei* stellar nerve showing the diffusion of thorium dioxide in the minute fibers. Thorium dioxide particles are observed in high concentration in the endoneurium (*E*) and appear bound to some dense material. Particles are also observed in the mesaxon gaps (arrows) and distributed in the spaces separating the axolemma of neighbor axons (*A*). Pinocytotic vesicles (*P*) containing thorium dioxide are seen in the Schwann cell cytoplasm (*SC*). OsO_4-fixed, Epon-embedded material.

cles was high at the endoneurium, mesaxon gaps, and axon–Schwann cell space (Figs. 3 and 4). On the other hand, in the giant nerve fiber, in spite of the high concentration of particles observed at the endoneurium, their concentration in the basement membrane was low and only few of the smallest particles were observed in the channel lumina and along the axon–Schwann cell space (Fig. 5). These results gave direct evidences on the permeability of the pathways crossing the Schwann cell layer and of the space surrounding the axolemma (9). Similar results were later reported by Baker (10) in crab nerve.

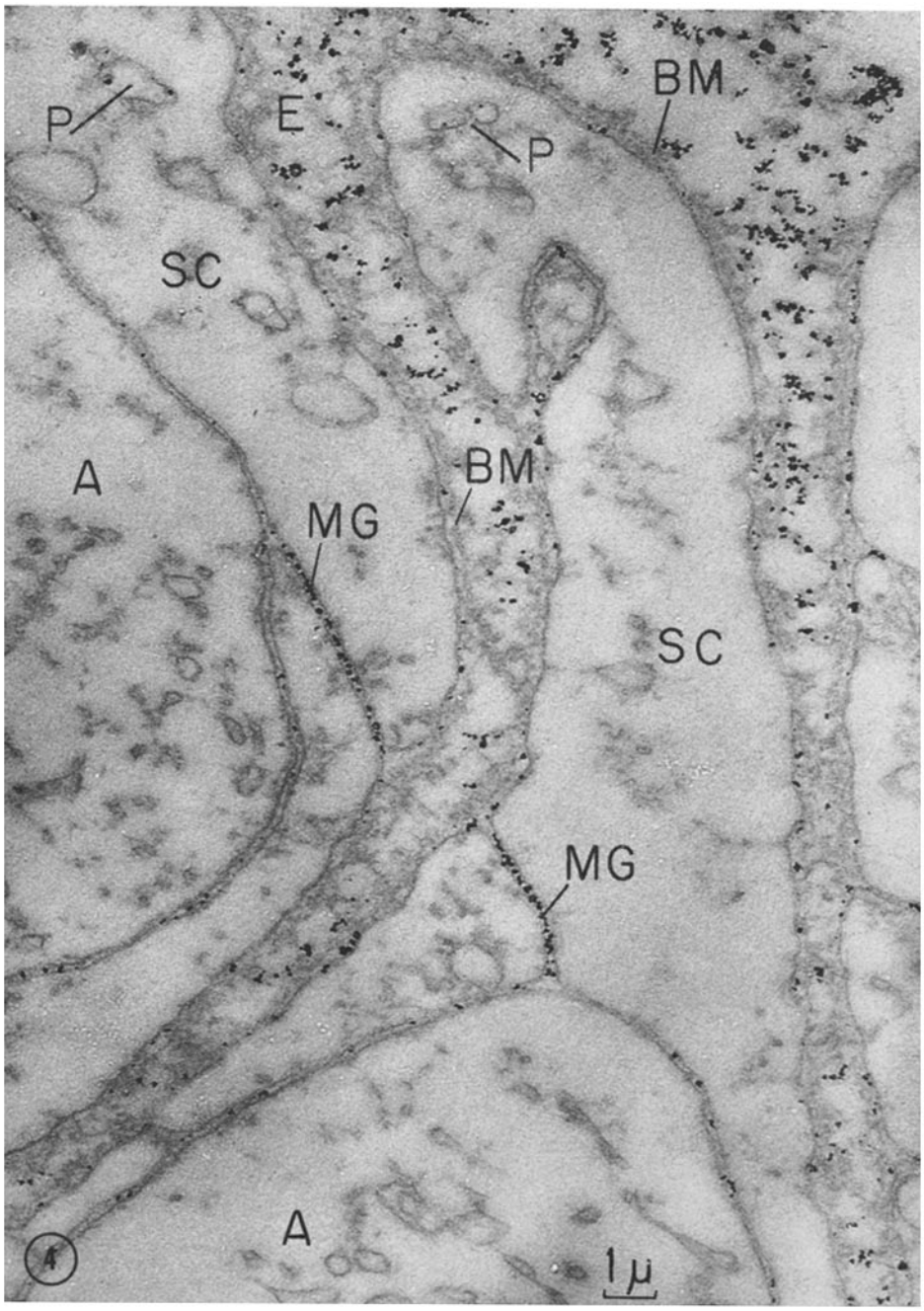

FIGURE 4. Electron micrograph of *D. plei* stellar nerve showing the diffusion of thorium dioxide in the medium-sized fibers. Notice the high concentration of thorium micelles bound to the endoneurial (*E*) dense material and in the mesaxon gaps (*MG*). Particles are also observed in the space separating the axon (*A*) from its Schwann cell (*SC*) and housed in pinocytotic vesicles (*P*) in the Schwann cell cytoplasm. A thin basement membrane (*BM*) lines the Schwann cell outer surface. Same material as in Fig. 2.

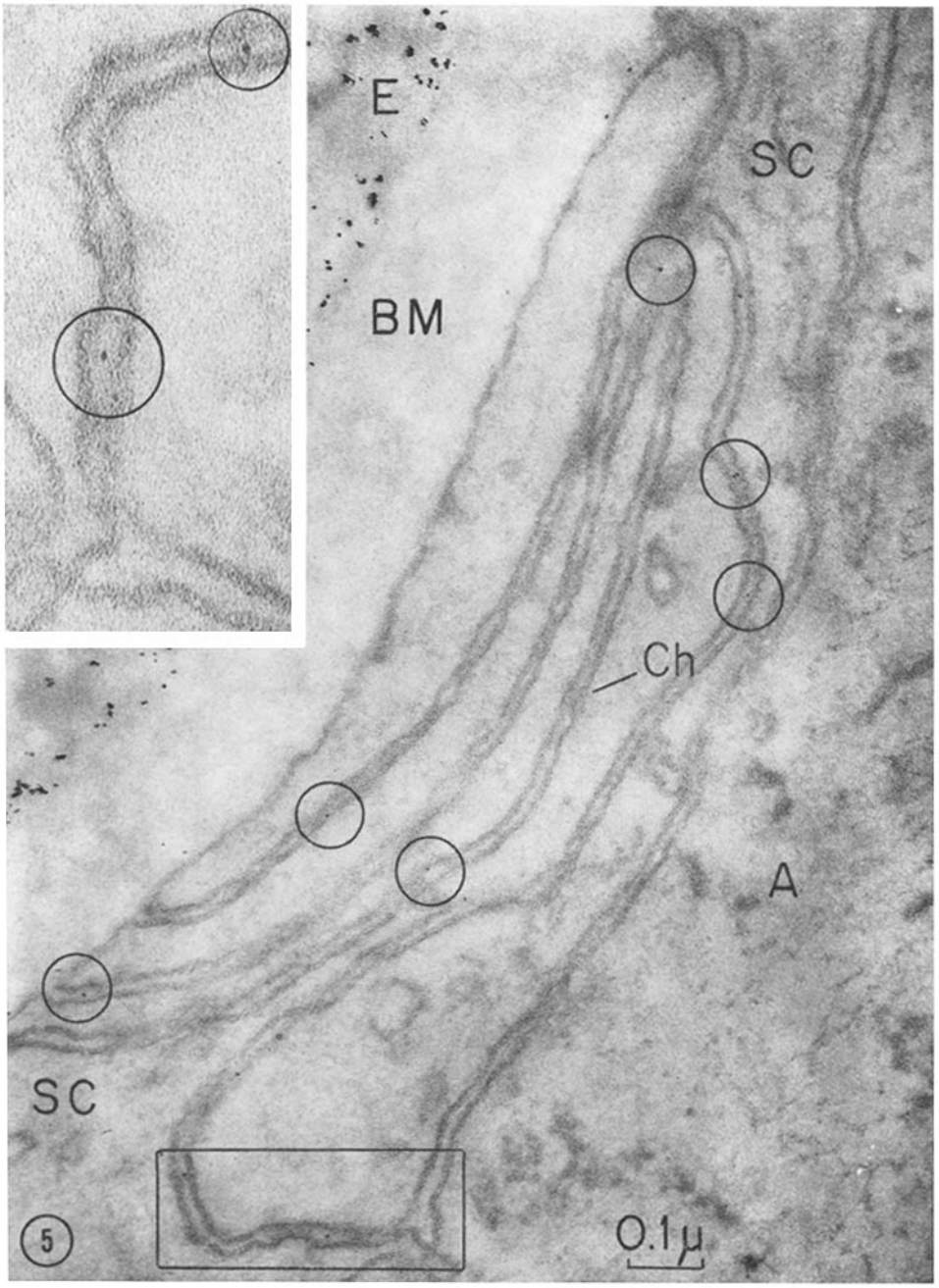

FIGURE 5. Electron micrograph of *D. plei* stellar nerve showing the diffusion of thorium dioxide in the giant fiber. Micelles of different sizes are observed in the endoneurium (*E*) while in the basement membrane (*BM*) practically disappear. A few particles of the smallest diameters are observed at the Schwann cell outer surface, channel (*Ch*) lumina and reaching the space between the axon (*A*) and the Schwann cell (*SC*). Insert is a blow-up of the area in the rectangle. Same material as in preceding figure.

The low concentration of thorium dioxide particles found in the basement membrane and channels of the giant nerve fiber, may be considered an indication either that the basement membrane is a barrier for the thorium particles or that they are trapped in the endoneurium. The thorium particles appear clustered in the endoneurium, juxtaposed to dense patches of extracellular material; the clear zones among those patches are devoid of thorium particles.

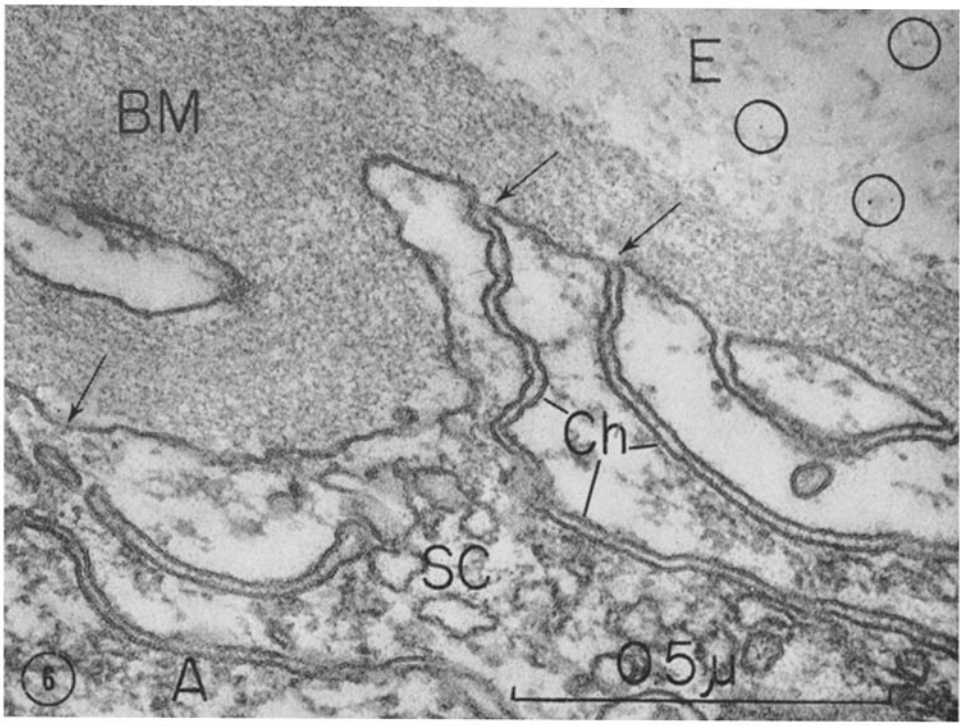

FIGURE 6. *D. Plei* giant fiber treated with hyaluronidase prior to the incubation in thorotrast. The basement membrane (*BM*) shows a granular appearance instead of the homogeneous one. Clear areas (arrows) are observed near the Schwann cell plasma membrane. The channel lumina (*Ch*) and axon–Schwann cell space present a low electron opacity. At the endoneurium (*E*) only scant, isolated particles of thorium dioxide are observed (circles). *A*, axon; *SC*, Schwann cell. OsO_4-fixed, Epon-embedded material.

Prior treatment of the nerve fibers with hyaluronidase (50 U/ml) during 1 hr, demonstrated that the basement membrane had lost its homogeneity and appeared to have been formed instead by a finely granular, dense material scattered on a clear background (Fig. 6). Low electron-opaque areas separated the fine, granular material from the Schwann cell plasma membrane. The channel lumina and axon–Schwann cell space presented also low electron opacity. When live hyaluronidase-treated nerve fibers were incubated in the sea water containing thorium dioxide, the electron microscope examination revealed that entry of particles into the Schwann cell chan-

nels and periaxonal space diminished and that the thorium micelles remained mainly in the endoneurium, farther outside the basement membrane than in the untreated nerve fibers (Fig. 6). Revel (11) has demonstrated that acid polysaccharides bind colloidal thorium. In addition, the penetration of mannitol in *D. plei* giant axons also decreases when the tissue is treated with hyaluronidase (unpublished data).

These results led us to study the polysaccharides in the squid nerve fiber. The

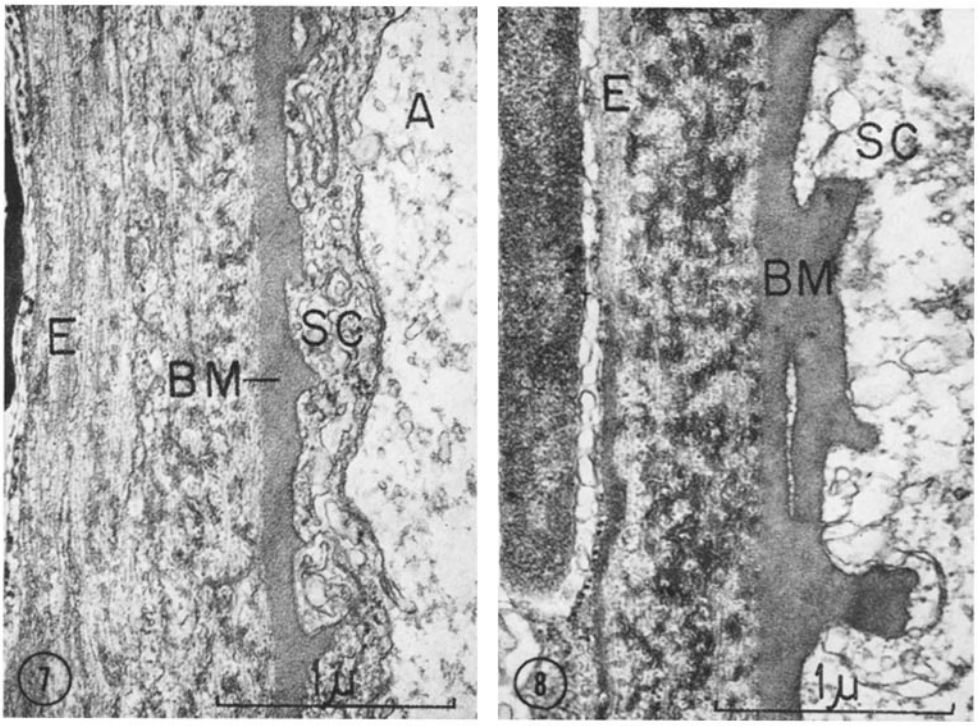

FIGURES 7 and 8. *D. plei* giant fibers treated with periodic acid–thiosemicarbazide–osmic acid (Seligman et al. method) before embedment for demonstrating mucopolysaccharides. Fig. 7 corresponds to a 200 μ giant axon while Fig. 8 corresponds to a 400 μ giant axon. Basement membranes (*BM*) show a positive reaction and also the material deposited in the endoneurium (*E*). Notice that this dense material is more abundant in the larger fiber than in the smaller one. *A*, axon; *SC*, Schwann cells.

method of Seligman et al. (12) was used at first. It consists of a histochemical reaction for demonstrating aldehydic groups liberated from the polysaccharides by the periodic acid; the free aldehyde groups are then combined with thiosemicarbazide or thiocarbohydrazyde to form a compound which selectively binds osmium tetroxide. This compound appears at the electron microscope as a material of high electron opacity.

Two groups of nerve fibers of squid *D. plei*, one group with diameters of about 200 μ and the other with diameters of about 400 μ, were studied after the treatment with the Seligman method performed in block, before embedding, or in fine sections

after embedding. Some damage of the structure due to the nature of the method was observed. However, the preservation was sufficient to demonstrate and locate positive material in the channel lumina and axon–Schwann cell space (Fig. 9). This fact was more evident in the nerve fibers treated after embedding (Fig. 10). The

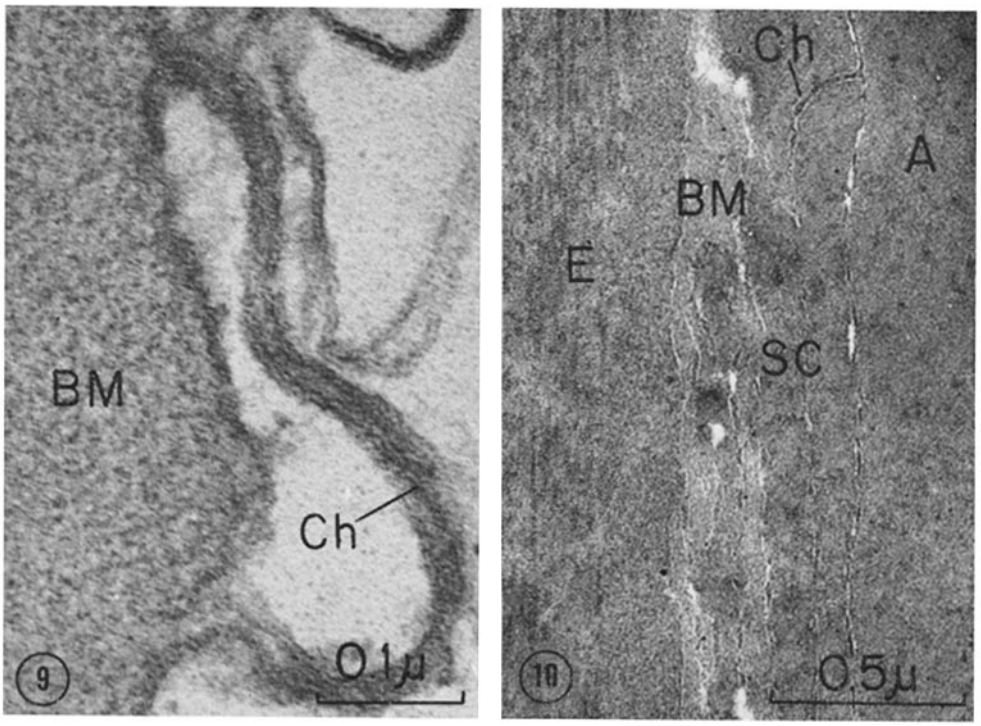

FIGURE 9. High-magnification electron micrograph of a channel (*Ch*) of the Schwann-cell layer of a giant fiber treated as stated in the preceding figures. Notice the positive reaction of the material filling the channel lumen. *BM*, basement membrane.

FIGURE 10. Electron micrograph of a smaller giant fiber of *D. plei* fixed in glutaraldehyde and embedded in Epon. The Seligman et al. method, as said for the preceding figures, was performed in fine sections. The nonstainability of the membranes, in this case, shows distinctively the positive material contained in the channel lumina (*Ch*) and axon–Schwann cell space. *A*, axon; *SC*, Schwann cell; *BM*, basement membrane; *E*, endoneurium.

basement membrane was also positive and more dense in the fibers with larger diameters than in the smaller ones (Figs. 7 and 8). Dark areas of positive material were also observed outside the basement membrane. These dark areas are more numerous and of higher density in the large fibers than in the small nerve fibers (Figs. 7 and 8).

The silver nitrate–hexamethylenetetramine method (13) was also used for observing the macromolecules laying outside the plasma membranes of the squid giant nerve

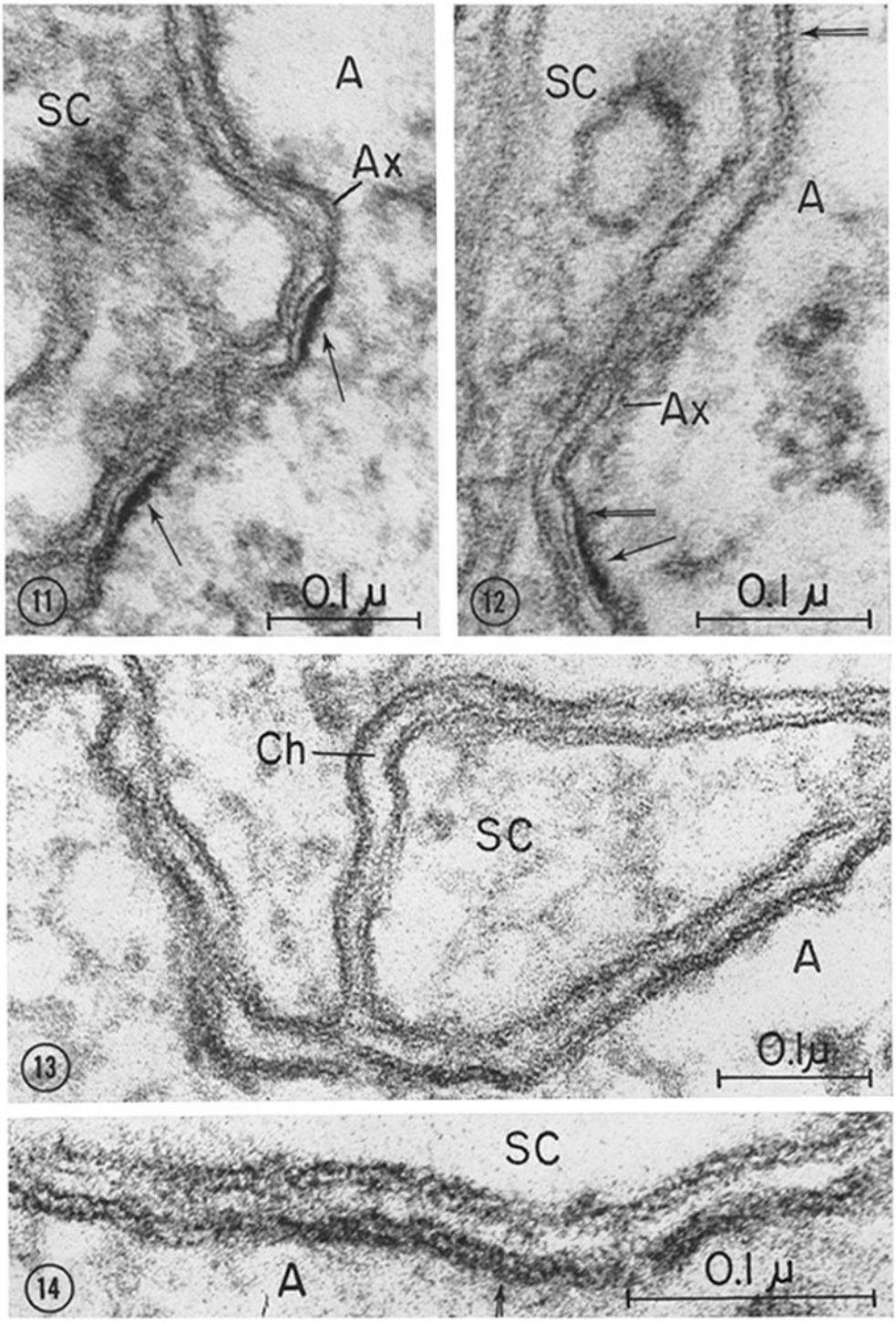

FIGURES 11–14. High-magnification electron micrographs of boundary between giant axon (*A*) and Schwann cell (*SC*). Schwann cell plasma membrane, channel wall (*Ch*), and axolemma (*Ax*) show three-layered continuous pattern and areas with septa placed among external and internal dense zones of membrane (double-stemmed arrows). In some regions (Fig. 14) favorable orientation of section permits easy identification of globular units in septated regions. Cytoplasmic densities (arrows), closely apposed to internal dense zone of axolemma are observed spaced along membrane. OsO_4-fixed, Epon-embedded material.

fibers. The results show that only the basement membrane is highly positive. This positivity turns negative in the control reaction performed without periodic acid.

THE STRUCTURE OF THE AXOLEMMA

The axolemma, or plasma membrane of the axon, measures 85–105 A across and presents the three-layered pattern that characterizes cell membranes as observed

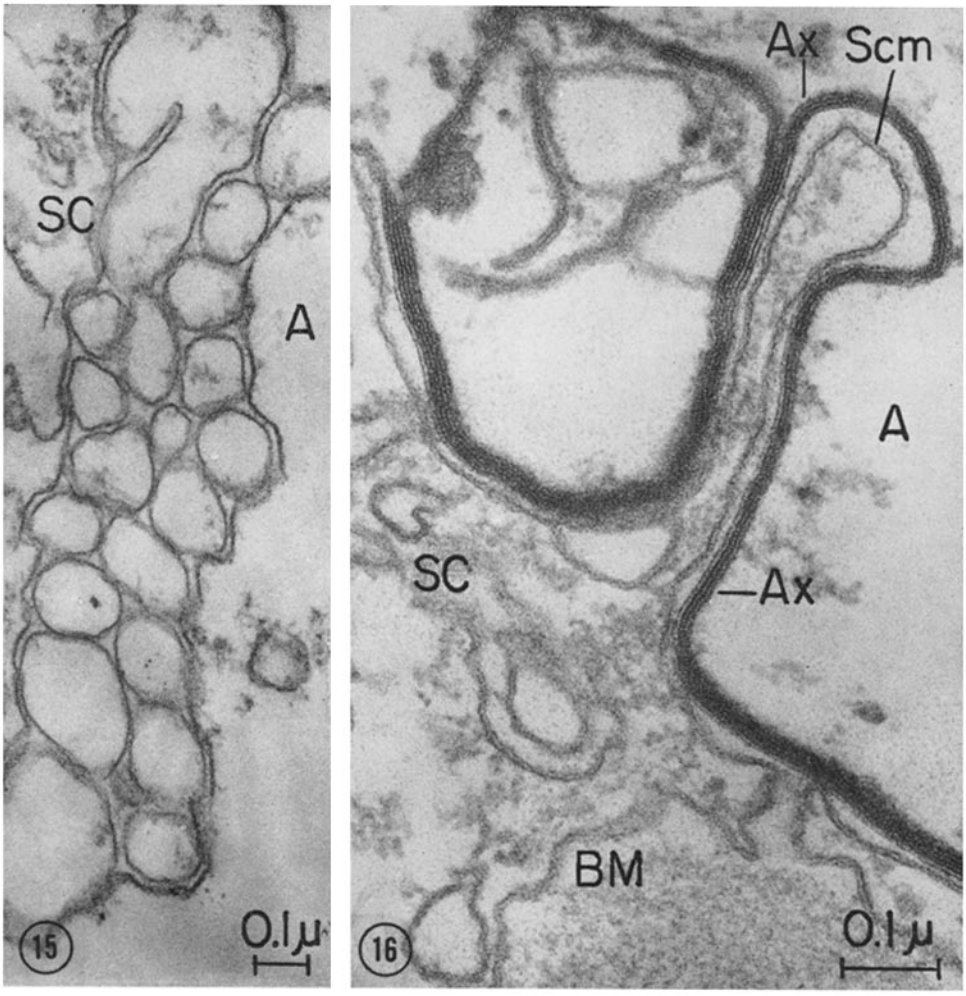

FIGURE 15. Giant fiber incubated during 15 min with 4 mM sodium lauryl sulfate. The boundary between the axon (*A*) and the Schwann cell is occupied by a group of membranous bubbles.

FIGURE 16. Electron micrograph of the same material as in Fig. 15 showing part of the axon (*A*), Schwann cell (*SC*), and basement membrane (*BM*) of a giant fiber. The axolemma (*Ax*) is replaced by a myelin-like sheath while the Schwann cell plasma membrane (*Scm*) does not show the same alteration.

with the electron microscope. The internal dense zone of the membrane, which is directly apposed to the axoplasm, is thicker than the external dense zone. In addition, local thickenings attached to the internal dense zone and almost regularly spaced along the membrane have been observed in the three species of squid studied (Figs. 11 and 12). These thickenings measure 400–800 A in length by 50–90 A across and remain in the nerves treated with hyaluronidase. The local thickenings resemble the so-called postsynaptic densities (14, 15) which has been assumed to be the point of transmission. Elfvin (16), Andres (17), and Peters (18) have shown cytoplasmic densities close to the axolemma in the Ranvier nodes of the peripheral and central nervous system and have related these densities to the permeability of the membrane at those points (16), to areas of activity (18), or to diffusion barriers (17). Sabatini,

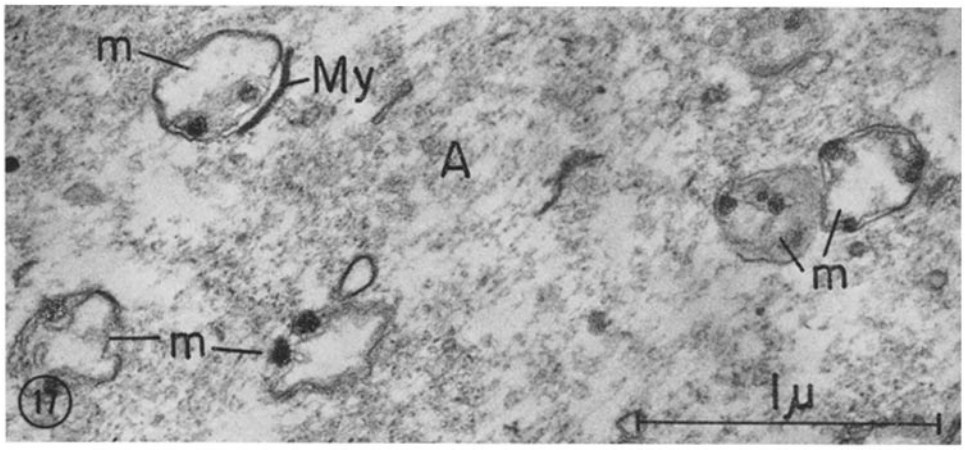

FIGURE 17. Axoplasm of a giant axon treated during 4 min with 4 mM sodium lauryl sulfate. Mitochondrial (*m*) alterations consist of myelin-like sheath (*My*) replacing zones of the outer membrane, and dense, round depots associated with the inner membrane and remnants of cristae.

Di Polo, and Villegas[1] have shown in the axolemma, areas of ATPase activity with the aid of histochemical techniques. These areas are spaced along the membrane. The local thickenings of the axolemma observed in the giant nerve fiber and the local regions of ATPase activity suggest that only certain areas of the membrane are able to accomplish specific functions.

In the last 5 yr several reports tend to demonstrate a closely packed micellar arrangement for the so-called unit membrane (19–21). In high-resolution electron micrographs, membranes appear to be formed by globular components separated by dense septa. On this basis Sjöstrand (22) has proposed a globular arrangement of the lipid micelles which form the membranes of the mitochondria and smooth cytoplasmic membranes. The protein chains would cover the surface of the micelles and prevent them from fusing into a continuous layer. Green and Perdue (27) have

[1] Sabatini, M. T., R. Di Polo, and R. Villegas. ATPase activity in the membranes of the squid nerve fiber. Submitted for publication.

also proposed that the membrane structure is formed by systems of lipoprotein-repeating units, each membrane having its own specific repeating unit regarding shape or size. The arrangement of lipid micelles found in model systems (23, 24) is compatible with the existence of water-filled pores in the membrane (25, 26).

The electron microscope examination of the squid nerve fibers shown in the present work demonstrates the existence of septa across the clear central zone of the plasma membranes of both the axon and the Schwann cell (Fig. 13). Globular units, 60–70 A in diameter, were distinguished between the septa (Fig. 14). These septa occur only at certain regions of the membrane, together with regions where the three-layered continuous pattern is observed. The septa have been observed mainly in regions different from those having the local thickenings (Figs. 11 and 12).

Raizin, Morowitz, and Terry (28) used detergent to dissolve the membrane of *Mycoplasma laidlawii*, the separated units then reaggregated when the detergent was removed and cations were added.

An attempt was made to separate the observed globular units of the squid axolemma by means of detergent. Nerve fibers of *D. Plei* were immersed in a 4 mM sodium lauryl sulfate solution prepared in artificial sea water. The recorded action potential disappeared rapidly, within 2 min of exposure to the detergent. The nerve fibers were then fixed for electron microscopy after 4, 15, and 45 min of immersion in the test solution. The alterations observed consisted of (*a*) the formation of zones of conglomerated membranous bubbles in the Schwann cell–axon boundary (Fig. 15) that might be formed by elongation of the axolemma and Schwann cell plasma membrane which have to pleat in order to occupy a more reduced area, and (*b*) the appearance of multilayered periodic structures, similar to the so-called myelin figures, involving the axolemma and the mitochondrial surface (Figs. 16 and 17).

At certain regions, the axolemma and the outer membrane of the axonnal mitochondria are substituted by a myelin-like sheath formed by four, six, or more dense lines with a regular spacing of 50–60 A between them. In the peripheral region of the axoplasm, the multilaminated structures may appear connected to the multilaminated sheath replacing the axolemma. Other periodical structures observed did not present the regular spacing, but they appear to be formed either by components of two fused membranes, each component measuring 120–150 A across and exhibiting one thicker, dense line in the center, or by apposition of unit membranes, about 80 A thick, separated by spaces 100 A across. Dense masses, in which a fine period of 35–40 A was discernible, were also observed at some places in connection with the multilaminated sheaths.

At the regions where the multilaminated figures were not seen, the axolemma shows the three-layered pattern and the septa observed in the untreated nerve fibers. (Figs. 18–20). After 45 min these regions appeared blurred, but disaggregation of the subunits was not observed (Fig. 21).

It is worth mentioning the striking difference observed between the behavior of the axolemma and the Schwann cell membranes (plasma membrane and channel walls). The multilaminated sheaths and myelin figures seem to be formed from the axolemma, while the Schwann cell plasma membrane and channel walls do not show the same alterations. After 15 min incubation, the Schwann cell appeared swollen and the channels dilated, but the membranes themselves still showed the

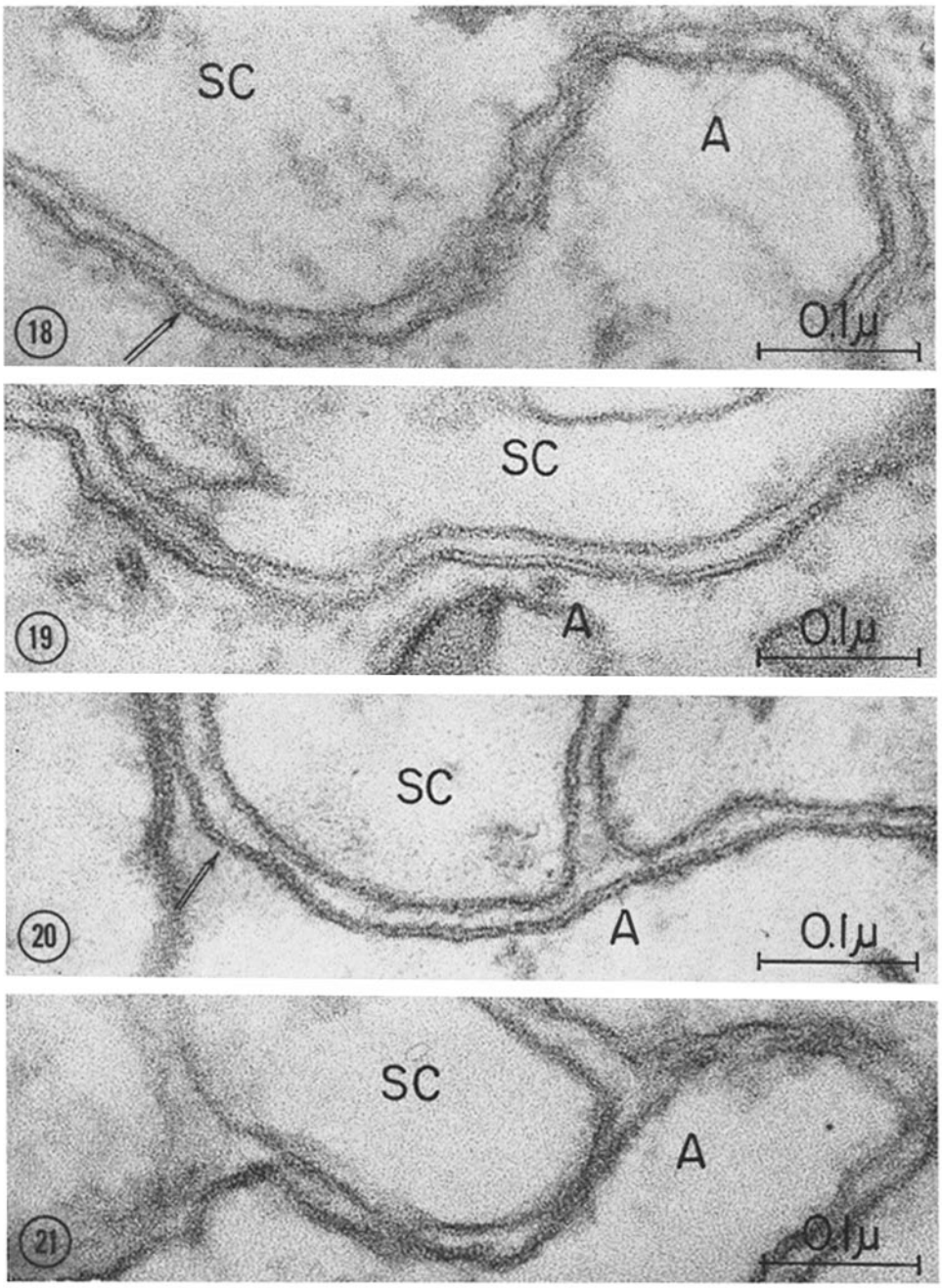

FIGURES 18–21. Boundary between the axon (*A*) and the Schwann cell (*SC*) of giant fibers treated during 4 (Figs. 18 and 19), 15 (Fig. 20), and 45 min (Fig. 21) in 4 mM sodium lauryl sulfate. In these specimens, electron micrographs present areas of the plasma membranes of axons and Schwann cells showing the continuous three-layered pattern or the septated pattern (double-stemmed arrows) observed in nontreated specimens. After 45 min incubation in the detergent (Fig. 21) it is noted a blurred appearance of the membranes.

normal pattern (Fig. 16). Only in the 45-min incubated specimens, numerous vacuoles, with multilaminated walls replaced the channels, and myelin figures appeared in the Schwann cytoplasm.

Since the lauryl sulfate was placed at the outside of the nerve fibers and the alterations appeared first in the axon, it may be considered as an indication that the axolemma, as well as the membranes of the axonnal mitochondria, are more susceptible to the action of the detergent than the Schwann cell membranes. This may be due to a different lipidic composition or to a different arrangement of the lipids and protein forming these membranes.

CONCLUSIONS

The results herein presented indicate that the systems of pathways on the nerve fiber surface (endoneurial spaces, mesaxon gaps, lumina of the Schwann layer channels, and axolemma–Schwann cell spaces) are permeable and allow the diffusion of particles as large as those of thorium dioxide. However, these pathways are not empty spaces but are occupied by a material which gives positive reaction to the histochemical methods for mucopolysaccharides and binds, to a certain extent, the thorium dioxide micelles. This extracellular material is present in small and giant axons. In the latter, the higher electron opacity observed in the giant axons with larger diameter ($\sim$400 μ in diameter), after use of the histochemical methods, indicates a higher concentration of mucopolysaccharides in those axons. This electron-opaque material appears to restrict diffusion, as is indicated by the difference between the concentrations of thorium dioxide particles in the mesaxon gaps of the small fibers and channels of the giant nerve fibers. Nevertheless, the normal structural organization of the mucopolysaccharides seems to provide a necessary medium for diffusion, since previous treatment with hyaluronidase restricts even more the entry of particles to the basement membrane, gaps, channels, and periaxonnal space.

The plasma membrane of the axon or axolemma presents, after the usual treatment for electron microscope observation, an asymmetric three-layered pattern which at certain zones appears to be divided by septa into globular-repeating units. At present it is not possible to say how frequently these septated areas occur along the membrane. It is tempting to suggest that they are specific pathways for some of the substances to move across the axolemma.

There are local thickenings of the internal zone of the axolemma that resemble the densities observed in the postsynaptic cytoplasm and Ranvier nodes. There are also local areas of ATPase activity in the axolemma.[1] We have also shown that detergents alter the axolemma only at certain regions. Therefore, one might consider the axolemma not as a homogenous membrane but as a mosaic formed by specific areas which accomplish different functions.

The authors wish to express their thanks to Messrs. J. Aristimuño and F. Paredes for their technical assistance, to Mr. R. Pingarrón for the photographic labor, and to Miss Arlette Dupré for the secretarial work. The drawings of Fig. 1 were made by Messrs. C. Quintero and J. Machin.

REFERENCES

1. YOUNG, J. Z. 1936. The structure of nerve fibres in Cephalopods and Crustacea. *Proc. Roy. Soc. (London) Ser. B.* **121**:319.

2. GEREN, B. B., and F. O. SCHMITT. 1954. The structure of the Schwann cell and its relation to the axon in certain invertebrate nerve fibers. *Proc. Natl. Acad. Sci. U. S.* **40**:863.
3. VILLEGAS, G. M., and R. VILLEGAS. 1960. The ultrastructure of the giant nerve fibre of the squid: axon–Schwann cell relationship. *J. Ultrastruct. Res.* **3**:362.
4. VILLEGAS, R., L. VILLEGAS, M. GIMENEZ, and G. M. VILLEGAS. 1963. Schwann cell and axon electrical potential differences. Squid nerve structure and excitable membrane location. *J. Gen. Physiol.* **46**:1047.
5. VILLEGAS, G. M. 1963. Ultraestructura de la fibra nerviosa gigante del calamar. *Acta Cient. Venezolana.* **1** (Suppl.):11.
6. VILLEGAS, G. M., and R. VILLEGAS. 1963. Morphogenesis of the Schwann channels in the squid nerve. *J. Ultrastruct. Res.* **8**:197.
7. GASSER, H. S. 1955. Properties of dorsal root undulated fibers on the two sides of the ganglion. *J. Gen. Physiol.* **38**:709.
8. DE LORENZO, A. J. 1957. Electron microscopy observations of the olfactory mucosa and olfactory nerve. *J. Biophys. Biochem. Cytol.* **3**:839.
9. VILLEGAS, G. M., and R. VILLEGAS. 1964. Extracellular pathways in the peripheral nerve fibre: Schwann cell layer permeability to thorium dioxide. *Biochim. Biophys. Acta.* **88**:231.
10. BAKER, P. F. 1965. A method for the location of extracellular space in crab nerve. *J. Physiol. (London).* **180**:439.
11. REVEL, J. P. 1964. A stain for the ultrastructural localization of acid mucopolysaccharides. *J. Microscop.* **3**:535.
12. SELIGMAN, A. M., J. S. HANKER, H. WASSERKING, H. DMOCHOWSKI, and L. KATZOFF. 1965. Histochemical demonstration of some oxidized macromolecules with thiocarbohydrazide (TCH) or thiosemicarbazide (TSC) and osmium tetroxide. *J. Histochem. Cytochem.* **13**:629.
13. RAMBOURG, A., and C. P. LEBLOND. 1967. Electron microscope observations on the carbohydrate-rich cell coat present at the surface of cells in the rat. *J. Cell Biol.* **32**:27.
14. PALAY, S. L. 1958. The morphology of synapses in the central nervous system. *Exptl. Cell Res. Supp. 5.* 275.
15. GRAY, E. J. 1959. Axo-somatic and axo-dendritic synapses of the cerebral cortex: an electron microscope study. *J. Anat.* **93**:420.
16. ELFVIN, L. G. 1961. The ultrastructure of the nodes of Ranvier in cat sympathetic nerve fibers. *J. Ultrastruct. Res.* **5**:374.
17. ANDRES, K. H. 1965. Über die Feinstruktur besonderer Einrichtungen in markhaltigen Nervenfasern des Kleinhirns der Ratte. *Z. Zellforsch. Mikroskop. Anat.* **65**:701.
18. PETERS, A. 1966. The node of Ranvier in the central nervous system. *Quart. J. Exptl. Physiol.* **51**:229.
19. BANGHAM, A. D., AND R. W. HORNE. 1962. Action of saponin on biological cell membranes. *Nature.* **196**:952.
20. GLAUERT, A. M., J. T. DINGLE, and J. A. LUCY. 1962. Action of saponin on biological cell membranes. *Nature.* **196**:953.

21. LUCY, J. A. 1964. Globular lipid micelles and cell membranes. *J. Theoret. Biol.* **7**:360.
22. SJÖSTRAND, F. S. 1963. A new ultrastructural element of the membranes in mitochondria and of some cytoplasmic membranes. *J. Ultrastruct. Res.* **9**:340.
23. LUZATTI, V., and F. HUSSON. 1962. The structure of the liquid-crystalline phases of lipid-water systems. *J. Cell Biol.* **12**:207.
24. STOECKENIUS, W. 1962. Some electron microscopical observations on liquid-crystalline phases in lipid-water systems. *J. Cell Biol.* **12**:221.
25. SOLOMON, A. K. 1960. Red cell membrane structure and ion transport. *J. Gen. Physiol.* **43**:(5, Pt. 2):1.
26. VILLEGAS, R. and F. V. BARNOLA. 1961. Characterization of the resting axolemma in the giant axon of the squid. *J. Gen. Physiol.* **44**:963.
27. GREEN, D. E. and J. F. PERDUE. 1966. Membranes as expressions of repeating units. *Proc. Natl. Acad. Sci. U. S.* **55**:1295.
28. RAIZIN, S., H. J. MOROWITZ, and T. M. TERRY. 1965. Membrane subunits of *Mycoplasma laidlawii* and their assembly to membranelike structures. *Proc. Natl. Acad. Sci. U. S.* **54**:211.